Quantum criticality and first-order transitions in the extended periodic Anderson model

I. Hagymási,[1,2] K. Itai,[1] and J. Sólyom[1]

[1]*Strongly Correlated Systems "Lendület" Research Group, Institute for Solid State Physics and Optics, MTA Wigner Research Centre for Physics, Budapest H-1525 P.O. Box 49, Hungary*

[2]*Institute of Physics, Eötvös University, Budapest, Pázmány Péter sétány 1/A, H-1117, Hungary*

We investigate the behavior of the periodic Anderson model in the presence of $d-f$ Coulomb interaction (U_{df}) using mean-field theory, variational calculation, and exact diagonalization of finite chains. The variational approach based on the Gutzwiller trial wave function gives a critical value of U_{df} and two quantum critical points (QCPs), where the valence susceptibility diverges. We derive the critical exponent for the valence susceptibility and investigate how the position of the QCP depends on the other parameters of the Hamiltonian. For larger values of U_{df}, the Kondo regime is bounded by two first-order transitions. These first-order transitions merge into a triple point at a certain value of U_{df}. For even larger U_{df} valence skipping occurs. Although the other methods do not give a critical point, they support this scenario.

I. INTRODUCTION

Heavy-fermion compounds often show remarkable phenomena like unconventional superconductivity or an unusual Fermi-liquid state. It turned out that in those compounds, for instance, CeIn$_3$,[1] whose superconducting state is unconventional, the pairing between electrons is mediated by antiferromagnetic spin fluctuations. The superconducting phase is formed near the antiferromagnetic quantum critical point (QCP)[2] as the pressure or, in other cases, the concentration of a component is varied. However, this theory seems to be insufficient to explain the temperature-pressure phase diagram of CeCu$_2$Ge$_2$ or CeCu$_2$Si$_2$, where a superconducting dome with enhanced transition temperature is located far away from the antiferromagnetic critical point. Since this discovery, these compounds have drawn much attention both experimentally and theoretically. It has been argued that this phenomenon is related to the critical valence fluctuations of Ce ions,[3–14] that is, to the existence of a second QCP.

The simplest model of heavy-fermion compounds is the periodic Anderson model (PAM).[15] It is known, however, that the mixed-valence regime appears always in this model as a smooth crossover, and valence fluctuations do not become critical for any choice of the parameters. A local Coulomb interaction between the conduction and localized electrons is needed for the appearance of a sharp transition and critical valence fluctuations.[4,11] The Hamiltonian of this extended periodic Anderson model can be written using standard notations in the following form:

$$\mathcal{H} = \sum_{\boldsymbol{k},\sigma} \varepsilon_d(\boldsymbol{k}) \hat{d}^{\dagger}_{\boldsymbol{k}\sigma} \hat{d}_{\boldsymbol{k}\sigma} - V \sum_{j,\sigma} (\hat{f}^{\dagger}_{j\sigma} \hat{d}_{j\sigma} + \hat{d}^{\dagger}_{j\sigma} \hat{f}_{j\sigma})$$
$$+ \varepsilon_f \sum_{j,\sigma} \hat{n}^f_{j\sigma} + U_f \sum_j \hat{n}^f_{j\uparrow} \hat{n}^f_{j\downarrow} + U_{df} \sum_{j,\sigma,\sigma'} \hat{n}^f_{j\sigma} \hat{n}^d_{j\sigma'}.$$

$$(1)$$

After Onishi and Miyake's pioneering work,[4] recently, this model has been investigated by several modern techniques, including density matrix renormalization group,[9] dynamical mean field,[16–18] variational calculations,[4,19] projector-based

renormalization approach,[20] and fluctuation exchange approximation.[21] It has been found that a first-order valence transition and a QCP may appear due to U_{df}.

Previous calculations[4,16,19] focused on the properties at infinite or large U_f. Mainly the existence of a QCP and the possibility of first-order transition was addressed. Our main goal here is to study the critical behavior for arbitrary values of U_f. We investigate how the QCP and the ε_f–U_{df} phase diagram depend on the parameters of the model in the half-filled case. In our previous paper[22] we have shown that the Gutzwiller's variational method gives reliable results concerning the valence; therefore, it is worth studying the valence transition by use of this method.

It is worth noting that a first-order transition from Mott insulator to Kondo insulator has been found[23] in a model with a more general Hamiltonian, too, including Hund's coupling and interaction between d electrons. We do not consider the Hund's coupling here since the appearance of critical valence fluctuations was attributed to the direct Coulomb interaction between d and f electrons.[4,11] The exchange coupling between them probably plays a minor role in this respect.

Note that in a previous paper of ours[24] a variational approach was formulated for another kind of extended periodic Anderson model, where a different form was chosen for the $d-f$ interaction, a spin-dependent four-body term. Neither a QCP, nor a first-order valence transition has been found in that model.

The setup of the paper is as follows. In Sec. II, we perform a mean-field calculation to demonstrate in the simplest way how U_{df} affects the intermediate valence regime. In Sec. III, the variational approach is introduced, which is based on the Gutzwiller wave function. We analyze the quantum critical behavior and the disappearance of the Kondo regime at a triple point. Moreover, we construct the ε_f–U_{df} phase diagram. In Sec. IV, we carry out exact diagonalization to investigate the model in one dimension and compare the results with that of mean-field theory and the Gutzwiller approach. Finally, in Sec. V, our conclusions are presented.

II. MEAN-FIELD CALCULATION

First, we will study the problem by mean-field methods. In this approach some kind of order has to be assumed. We performed calculations by assuming two possibilities: (a) the system is paramagnetic; (b) it possesses a spatially oscillating magnetic order with a total magnetization zero. The state with lowest energy is accepted as the ground state. According to our calculations, the mean-field equations always have a paramagnetic solution, but in the Kondo regime, where localized moments are present, ordering of the moments leads to the lowering of the energy. We assume a simple cubic lattice in the following calculations, which can be partitioned into two sublattices (A and B). We expect that in the broken symmetry phase the electrons are ordered on the two sublattices in an alternating fashion, that is,

$$\langle \hat{n}^f_{j\sigma} \rangle = \tfrac{1}{2}[n_f + \sigma m_f e^{i\boldsymbol{q}_0 \cdot \boldsymbol{R}_j}], \tag{2}$$

where m_f is the magnetization of the sublattice and $\boldsymbol{q}_0 = \pi/a(1,1,1)$, so $\boldsymbol{q}_0 \boldsymbol{R}_j = 2\pi n$ on sublattice A and $\boldsymbol{q}_0 \boldsymbol{R}_j = (2n+1)\pi$ on sublattice B (n is an integer), and n_f is the average number of f electrons per site. The values of n_f and m_f need to be determined self-consistently. A similar oscillation can be assumed for the d electrons,

$$\langle \hat{n}^d_{j\sigma} \rangle = \tfrac{1}{2}[n_d + \sigma m_d e^{i\boldsymbol{q}_0 \cdot \boldsymbol{R}_j}], \tag{3}$$

although m_d will not appear explicitly in the calculations. The mean-field Hamiltonian is

$$\begin{aligned}
\mathcal{H}^m_{\mathrm{AF}} = &\sum_{\boldsymbol{k},\sigma}[\varepsilon_d(\boldsymbol{k}) + U_{df}n_f]\hat{d}^\dagger_{\boldsymbol{k}\sigma}\hat{d}_{\boldsymbol{k}\sigma} \\
&+ \sum_{j,\sigma}\left[\varepsilon_f + \frac{U_f}{2}(n_f - \sigma e^{i\boldsymbol{q}_0\cdot\boldsymbol{R}_j}m_f) + U_{df}n_d\right]\hat{n}^f_{j\sigma} \\
&+ V\sum_{j,\sigma}(\hat{f}^\dagger_{j\sigma}\hat{d}_{j\sigma} + \hat{d}^\dagger_{j\sigma}\hat{f}_{j\sigma}) \\
&- \frac{NU_f}{4}(n_f^2 - m_f^2) - NU_{df}n_fn_d,
\end{aligned} \tag{4}$$

where the $\boldsymbol{k}$ sum extends over the whole Brillouin zone of the simple cubic lattice and N is the number of sites. Due to the assumed magnetic ordering, the size of the Brillouin zone is reduced to half of its original size. In order to restrict the $\boldsymbol{k}$ sum to the magnetic Brillouin zone, we split the original sum into two parts by introducing the operators $\hat{d}^\dagger_{\boldsymbol{k}+\boldsymbol{q}_0\sigma}$ and $\hat{f}^\dagger_{\boldsymbol{k}+\boldsymbol{q}_0\sigma}$. We suppose that the dispersion relation possesses the nesting property

$$\varepsilon_d(\boldsymbol{k} + \boldsymbol{q}_0) = -\varepsilon_d(\boldsymbol{k}), \tag{5}$$

which is valid in a tight-binding model with nearest-neighbor hopping. This fixes the zero of the energy scale. The mean-field Hamiltonian then can be rewritten in Bloch representation,

$$\mathcal{H}^m_{\mathrm{AF}} = \sum_{\boldsymbol{k},\sigma}{}' \begin{pmatrix} \hat{d}_{\boldsymbol{k}\sigma} \\ \hat{d}_{\boldsymbol{k}+\boldsymbol{q}_0\sigma} \\ \hat{f}_{\boldsymbol{k}\sigma} \\ \hat{f}_{\boldsymbol{k}+\boldsymbol{q}_0\sigma} \end{pmatrix}^\dagger \mathcal{H}(\boldsymbol{k},\sigma) \begin{pmatrix} \hat{d}_{\boldsymbol{k}\sigma} \\ \hat{d}_{\boldsymbol{k}+\boldsymbol{q}_0\sigma} \\ \hat{f}_{\boldsymbol{k}\sigma} \\ \hat{f}_{\boldsymbol{k}+\boldsymbol{q}_0\sigma} \end{pmatrix} \\ - \frac{NU_f}{4}(n_f^2 - m_f^2) - NU_{df}n_fn_d, \tag{6}$$

where the prime denotes that the summation is carried out over the magnetic Brillouin zone, and

$$\mathcal{H}(\boldsymbol{k},\sigma) = \begin{pmatrix} \xi_d(\boldsymbol{k}) & 0 & V & 0 \\ 0 & \tilde{\xi}_d(\boldsymbol{k}) & 0 & V \\ V & 0 & \xi_f & -U_f\sigma m_f/2 \\ 0 & V & -U_f\sigma m_f/2 & \xi_f \end{pmatrix}, \tag{7}$$

where $\xi_f = \varepsilon_f + U_f n_f/2 + U_{df}n_d$, $\xi_d(\boldsymbol{k}) = \varepsilon_d(\boldsymbol{k}) + U_{df}n_f$ and $\tilde{\xi}_d(\boldsymbol{k}) = -\varepsilon_d(\boldsymbol{k}) + U_{df}n_f$. This Hamiltonian can be diagonalized by the unitary transformation $\mathcal{T}(\boldsymbol{k}\sigma)$, which is a real matrix in our case, leading to

$$\begin{aligned}
\mathcal{H}^m_{\mathrm{AF}} = &\sum_{\boldsymbol{k},\sigma}{}'\big[E_a(\boldsymbol{k})\hat{A}^\dagger_{\boldsymbol{k}\sigma}\hat{A}_{\boldsymbol{k}\sigma} + E_b(\boldsymbol{k})\hat{B}^\dagger_{\boldsymbol{k}\sigma}\hat{B}_{\boldsymbol{k}\sigma} \\
&+ E_c(\boldsymbol{k})\hat{C}^\dagger_{\boldsymbol{k}\sigma}\hat{C}_{\boldsymbol{k}\sigma} + E_d(\boldsymbol{k})\hat{D}^\dagger_{\boldsymbol{k}\sigma}\hat{D}_{\boldsymbol{k}\sigma}\big] \\
&- \frac{NU_f}{4}(n_f^2 - m_f^2) - NU_{df}n_fn_d, \tag{8}
\end{aligned}$$

where

$$(\hat{A}^\dagger_{\boldsymbol{k}\sigma}\ \hat{B}^\dagger_{\boldsymbol{k}\sigma}\ \hat{C}^\dagger_{\boldsymbol{k}\sigma}\ \hat{D}^\dagger_{\boldsymbol{k}\sigma}) = (\hat{d}^\dagger_{\boldsymbol{k}\sigma}\ \hat{d}^\dagger_{\boldsymbol{k}+\boldsymbol{q}_0\sigma}\ \hat{f}^\dagger_{\boldsymbol{k}\sigma}\ \hat{f}^\dagger_{\boldsymbol{k}+\boldsymbol{q}_0\sigma})\mathcal{T}^\dagger(\boldsymbol{k}\sigma). \tag{9}$$

The diagonalization is done numerically for each $\boldsymbol{k}$ value and we sort the eigenvalues in increasing order $[E_a(\boldsymbol{k}) \leqslant E_b(\boldsymbol{k}) \leqslant E_c(\boldsymbol{k}) \leqslant E_d(\boldsymbol{k})]$. Moreover, the eigenvalues have to be determined iteratively, since n_f, m_f, and n_d appearing in $\mathcal{H}(\boldsymbol{k},\sigma)$ have to satisfy a self-consistency condition. This condition can easily be formulated in the half-filled case, where—as it will be discussed below—the two lower bands with dispersion $E_a(\boldsymbol{k})$ and $E_b(\boldsymbol{k})$ are fully occupied and the two higher lying bands are empty. The conditions of self-consistency for n_f and m_f are

$$n_f = \frac{1}{N}\sum_{\boldsymbol{k},\sigma}{}'\big[\mathcal{T}^2_{31}(\boldsymbol{k}\sigma) + \mathcal{T}^2_{32}(\boldsymbol{k}\sigma) + \mathcal{T}^2_{41}(\boldsymbol{k}\sigma) + \mathcal{T}^2_{42}(\boldsymbol{k}\sigma)\big], \tag{10}$$

$$m_f = \frac{4}{N}\sum_{\boldsymbol{k}}{}'\big[\mathcal{T}_{31}(\boldsymbol{k}\uparrow)\mathcal{T}_{41}(\boldsymbol{k}\uparrow) + \mathcal{T}_{32}(\boldsymbol{k}\uparrow)\mathcal{T}_{42}(\boldsymbol{k}\uparrow)\big], \tag{11}$$

and the total energy is

$$\begin{aligned}
\mathcal{E}^{\mathrm{AF}}_g = &\sum_{\boldsymbol{k},\sigma}{}'[E_a(\boldsymbol{k}) + E_b(\boldsymbol{k})] \\
&- \frac{NU_f}{4}(n_f^2 - m_f^2) - NU_{df}n_fn_d. \tag{12}
\end{aligned}$$

Before evaluating the self-consistency equations, we return to the problem of the eigenvalue equations. Analytic expressions can be given at the symmetric point, and the obtained four bands for $U_{df} = 0$ become simply

$$\begin{aligned}
E_\alpha(\boldsymbol{k}) = &\pm\frac{1}{\sqrt{2}}\big[\varepsilon_d^2(\boldsymbol{k}) + U_f^2 m_f^2 + 2V^2 \\
&\pm \sqrt{(\varepsilon_d^2(\boldsymbol{k}) - U_f^2 m_f^2)^2 + 4V^2(\varepsilon_d^2(\boldsymbol{k}) + U_f^2 m_f^2)}\big]^{\frac{1}{2}}. \tag{13}
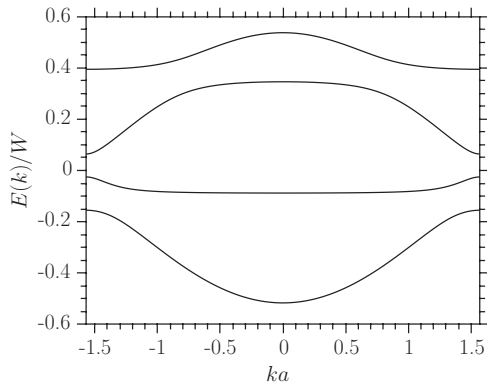\end{aligned}$$

FIG. 1. The dispersion curves of the states diagonalizing the mean-field Hamiltonian for $U_f/W = 0.5$, $U_{df}/W = 0$, $\varepsilon_f/W = -0.1$, $V/W = 0.1$.

The band structure is displayed in Fig. 1 for the one-dimensional tight-binding case for a special, but nonsymmetric, choice of the parameters. In higher dimensions, the system does not necessary remain insulating if the gap opens at different energies in different points of the zone boundary.

The self-consistency equations always have a paramagnetic solution, $m_f = 0$, and in certain cases they have a magnetic solution, $|m_f| > 0$. We compare the energies of both solutions and accept that one, which has lower energy. It is worth noting that the polarization of the d electrons, m_d, is also nonzero and its sign is opposite to m_f in the magnetic solution (though its value is smaller than m_f by an order of magnitude).

In the actual calculations we do not work in $\bm{k}$ space. The summations over $\bm{k}$ are carried out by assuming a constant density of states $\rho(\varepsilon) = 1/W$ in the interval $\varepsilon \in [-W/2, W/2]$. The same $\rho(\varepsilon)$ will be used in the variational calculation, too. The numerical results for n_f are shown in Fig. 2 for different values of U_{df}. As long as the f level is nearly fully occupied or empty, the paramagnetic solution is favorable, while when the occupancy is nearly 1, the magnetic solution has lower energy. For $U_{df}/W = 0$, the f level occupancy is continuous, although there is a discontinuity in its derivative at the point where the paramagnetic solution switches to magnetic or vice versa. This happens in Fig. 2 at $\varepsilon_f/W \approx -3.45$ and 0.45.
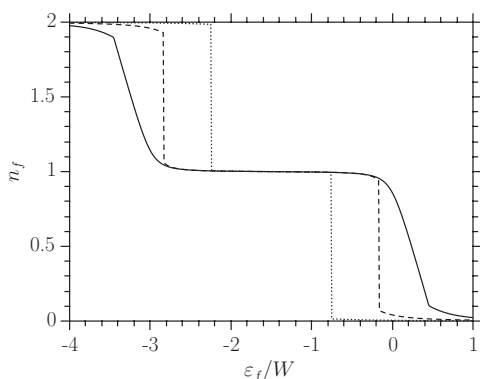

FIG. 2. The f-level occupancy as a function of ε_f obtained by mean-field theory. The solid, dashed, and dotted lines belong to $U_{df}/W = 0$, 0.4, 1, respectively, $V/W = 0.1$, $U_f/W = 3$ in all cases.

For increasing U_{df} values, first, the mixed-valence regime narrows, and then a jump, a first-order transition, appears in the f-level occupancy between the paramagnetic and the magnetic solution and the Kondo regime shrinks rapidly. This first-order transition has already been found by other calculations.[16,19] As is seen here, this simple mean-field approach can also account for it. The mean-field theory gives a critical value of $U_{df}^c/W \approx 0.26$ for $V/W = 0.1$, $U_f/W = 3$.

At a certain value of U_{df} above U_{df}^c the magnetic solution is stable in a single point, $\varepsilon_f = -U_f/2$. In this point the paramagnetic solutions with $n_f \approx 2$ and $n_f \approx 0$, and the magnetic solution with $n_f = 1$ have the same energy, that is, three states coexist. This is a triple point, since three first-order transition lines meet here. For larger U_{df} values, beyond the triple point, a so-called valence skipping occurs, that is, the valence state $n_f \approx 1$ is missing, since a direct first-order transition takes place from $n_f \approx 2$ to $n_f \approx 0$. It is interesting to note that so far the valence skipping (which was observed in several compounds, for example, $BaBiO_3$) has been attributed to the presence of a negative U_f.[25] As it is demonstrated here, large-enough U_{df} can also lead to valence skipping, even if $U_f > 0$. The mean-field theory gives $U_{df}^{triple}/W \approx 1.75$ for $V/W = 0.1$, $U_f/W = 3$. Note that this is in good agreement with the result $U_{df}^{triple} \approx U_f/2 + W/4$ that will be obtained by use of the Gutzwiller method.

This picture remains valid even when U_f is small, but finite, compared to the bandwidth. Although no plateau with $n_f \approx 1$ is formed, that is, there is no Kondo regime, a stable magnetic solution is found near the symmetric point, and this regime is bounded by first-order transitions above a finite U_{df}^c. Note that for $U_f/W = 0$ there is no triple point due to the lack of magnetic solution. However, a direct first-order transition appears between the paramagnetic states with solution between $n_f \approx 2$ and $n_f \approx 0$ above a certain value of U_{df}.

Although this theory gives a qualitatively good description of the first-order transition, there are several problems with it. First, we had to assume a magnetic order of spin-density-wave type, while no long-range order is expected in the Kondo regime. Second, the valence susceptibility, which is defined by

$$\chi_V = -\frac{dn_f}{d\varepsilon_f}, \qquad (14)$$

is not a continuous function, as is mentioned above, even below U_{df}^c/W, where n_f is continuous. The mean-field approach does not provide us with a critical point, where χ_V would diverge. In order to find a QCP and to investigate its properties, we need a more accurate calculation. This is done in the next section by use of the variational method.

III. VARIATIONAL CALCULATION

In what follows we generalize the variational approach used in Refs. 22 and 26 and summarize briefly the main steps of the calculation. We restrict ourselves to the paramagnetic case, that is, the number of up-spin and down-spin electrons are assumed to be equal locally, too. As it will be pointed out, the quantum criticality and the first-order transition appear

without any further assumptions, in contrast to the mean-field calculation. The trial state is expressed in terms of Gutzwiller projectors,

$$|\Psi\rangle = \hat{P}(f^1 d^2)\hat{P}(f^1 d^1)\hat{P}(f^2 d^2)\hat{P}(f^2 d^1)\hat{P}(f^2)|\Psi_0\rangle, \quad (15)$$

where

$$|\Psi_0\rangle = \prod_\sigma \prod_{\boldsymbol{k}}[u(\boldsymbol{k})\hat{f}_{\boldsymbol{k},\sigma}^\dagger + v(\boldsymbol{k})\hat{d}_{\boldsymbol{k},\sigma}^\dagger]|0\rangle \quad (16)$$

contains the mixing amplitudes $u(\boldsymbol{k})$ and $v(\boldsymbol{k})$ as variational parameters, and the sum over $\boldsymbol{k}$ extends over the whole Brillouin zone. The Gutzwiller projectors $\hat{P}(f^\alpha d^\beta)$, where α and β denote the f- and d-electron numbers, respectively, act on the on-site electron configurations defined by their arguments, making that configuration less probable. For example,

$$\hat{P}(f^2) = \prod_{\boldsymbol{g}}\big[1 - (1 - \eta(f^2))\hat{n}_{\boldsymbol{g}\uparrow}^f \hat{n}_{\boldsymbol{g}\downarrow}^f\big] \quad (17)$$

is the standard Gutzwiller projector for two f electrons on the same site. The other ones take into account correlations between d and f electrons, for example,

$$\hat{P}(f^1 d^2) = \prod_{\boldsymbol{g}}\big\{1 - (1 - \eta(f^1 d^2))\big[\hat{n}_{\boldsymbol{g}\uparrow}^f\big(1 - \hat{n}_{\boldsymbol{g}\downarrow}^f\big)$$
$$+ \hat{n}_{\boldsymbol{g}\downarrow}^f\big(1 - \hat{n}_{\boldsymbol{g}\uparrow}^f\big)\big]\hat{n}_{\boldsymbol{g}\uparrow}^d \hat{n}_{\boldsymbol{g}\downarrow}^d\big\}, \quad (18)$$

$$\hat{P}(f^2 d^2) = \prod_{\boldsymbol{g}}\big\{1 - (1 - \eta(f^2 d^2))\hat{n}_{\boldsymbol{g}\uparrow}^f \hat{n}_{\boldsymbol{g}\downarrow}^f \hat{n}_{\boldsymbol{g}\uparrow}^d \hat{n}_{\boldsymbol{g}\downarrow}^d\big\}. \quad (19)$$

The remaining projectors are defined straightforwardly. Besides the mixing amplitudes, we have five variational parameters, $\eta(f^2 d^2)$, $\eta(f^2 d^1)$, $\eta(f^1 d^2)$, $\eta(f^1 d^1)$, and $\eta(f^2)$, controlled by U_{df} and U_f. The tedious procedure of optimization is omitted here. Performing the optimization with respect to the mixing amplitudes using the Gutzwiller approximation, we obtain

$$\mathcal{E} = \frac{1}{N}\sum_{\boldsymbol{k}}\Big[q_d \varepsilon_d(\boldsymbol{k}) + \tilde{\varepsilon}_f - \sqrt{[q_d \varepsilon_d(\boldsymbol{k}) - \tilde{\varepsilon}_f]^2 + 4\tilde{V}^2}\Big]$$
$$+ (\varepsilon_f - \tilde{\varepsilon}_f)n_f + U_f v(f^2) + U_{df}\big[4v(f^2 d^2)$$
$$+ 2(v(f^2 d^1) + v(f^1 d^2)) + v(f^1 d^1)\big] \quad (20)$$

for the ground-state energy density, where $v(f^2)$ is the density of doubly occupied f sites. The other $v(f^\alpha d^\beta)$ quantities denote the corresponding densities of the $f^\alpha d^\beta$ configurations, e.g.,

$$v(f^1 d^2) = \frac{1}{N}\langle\big[\hat{n}_{\boldsymbol{g}\uparrow}^f\big(1 - \hat{n}_{\boldsymbol{g}\downarrow}^f\big) + \hat{n}_{\boldsymbol{g}\downarrow}^f\big(1 - \hat{n}_{\boldsymbol{g}\uparrow}^f\big)\big]\hat{n}_{\boldsymbol{g}\uparrow}^d \hat{n}_{\boldsymbol{g}\downarrow}^d\rangle,$$
$$v(f^2 d^2) = \frac{1}{N}\langle\hat{n}_{\boldsymbol{g}\uparrow}^f \hat{n}_{\boldsymbol{g}\downarrow}^f \hat{n}_{\boldsymbol{g}\uparrow}^d \hat{n}_{\boldsymbol{g}\downarrow}^d\rangle, \quad (21)$$

where $\tilde{V} = V\sqrt{q_f q_d}$ is the renormalized hybridization and q_f and q_d are the kinetic energy renormalization factors for the f and d electrons, respectively. Their analytic forms are now much longer than in our previous paper,[22] and after a tedious algebra we arrive at the following complete square forms:

$$q_f = \frac{1}{(n_f/2)[1 - (n_f/2)]}\Big[\sqrt{v(f^2 d^2)v(f^1 d^2)} + 2\sqrt{v(f^2 d^1)v(f^1 d^1)} + \sqrt{v(f^2 d^0)v(f^1 d^0)}$$
$$+ \sqrt{v(f^1 d^2)v(f^0 d^2)} + 2\sqrt{v(f^1 d^1)v(f^0 d^1)} + \sqrt{v(f^1 d^0)v(f^0 d^0)}\Big]^2, \quad (22)$$

$$q_d = \frac{1}{[(n/2) - (n_f/2)][1 - (n/2 + n_f/2)]}\Big[\sqrt{v(f^2 d^2)v(f^2 d^1)} + 2\sqrt{v(f^1 d^2)v(f^1 d^1)}$$
$$+ \sqrt{v(f^0 d^2)v(f^0 d^1)} + \sqrt{v(f^2 d^1)v(f^2 d^0)} + 2\sqrt{v(f^1 d^1)v(f^1 d^0)} + \sqrt{v(f^0 d^1)v(f^0 d^0)}\Big]^2, \quad (23)$$

where n is the band filling, which is 2 in our case. It is remarkable that the renormalized hybridization can still be written as the square root of q_f and q_d in the presence of U_{df}, too. Furthermore, $\tilde{\varepsilon}_f$, the quasiparticle energy level of f electrons, has the same form as in Ref. 22. It provides a self-consistency equation for n_f. The summation over $\boldsymbol{k}$ in Eq. (20) is carried out with a constant density of states, $\rho(\varepsilon) = 1/W$, in the interval $\varepsilon \in [-W/2, W/2]$. During the optimization process, the $\eta(f^\alpha d^\beta)$ variational parameters are expressed as functions of the quantities $v(f^\alpha d^\beta)$; therefore, the actual optimization can be done with respect to these parameters. All in all, the energy density given in (20) has to be optimized for n_f and $v(f^2)$, $v(f^2 d^1)$, $v(f^2 d^2)$, $v(f^1 d^1)$, and $v(f^1 d^2)$; the other quantities appearing in Eqs. (22) and (23) can be expressed using these due to the conservation of the number of particles. The evaluation of the variational equations could be done only numerically.

We first address what happens in the mixed-valence regime. As U_{df} is switched on, the mixed-valence regimes tend to

be sharper and sharper. This can be characterized by the valence susceptibility defined in Eq. (14) and displayed in Fig. 3 for different values of U_{df}. Note that in the half-filled case, this function is symmetric to the point $\varepsilon_f = -U_f/2$; therefore, it is sufficient to investigate the critical behavior in the regime $0 < n_f < 1$. In what follows, we focus on this regime, if not mentioned otherwise. It is found, in agreement with other calculations,[16,19] that χ_V diverges for a certain value of U_{df}^c and two values of ε_f^c related by the symmetry with respect to $-U_f/2$. These two points are identified as the QCPs. Following the maximum values of χ_V, the position of the QCP can be determined. We found that χ_V diverges as

$$\chi_V|_{\varepsilon_f = \varepsilon_f^c} \sim \frac{1}{|U_{df} - U_{df}^c|}, \quad (24)$$

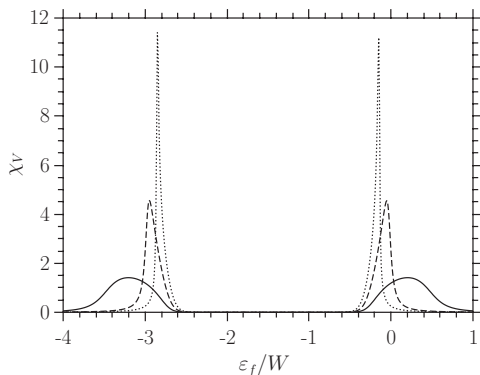$$\chi_V|_{U_{df} = U_{df}^c} \sim \frac{1}{|\varepsilon_f - \varepsilon_f^c|}. \quad (25)$$

FIG. 3. The valence susceptibility as a function of the f-level energy for $U_f/W = 3$ and $V/W = 0.1$. The solid, dashed, and dotted lines correspond to $U_{df}/W = 0$, 0.3, and 0.4, respectively.

This power-law behavior is valid for every choice of the parameters we used in our calculations, indicating universality.

Our Gutzwiller calculation makes it possible to investigate how the position of the QCP depends on U_f and V. In Fig. 4 the critical U_{df}^c and ε_f^c (for the QCP in the $0 < n_f < 1$ regime) are shown as a function of U_f for a fixed V. We found that (i) even for $U_f = 0$ there exists a critical point, (ii) U_{df}^c and ε_f^c vary monotonically as U_f increases, and (iii) both of them saturate as U_f reaches the value above which there exists a stable Kondo regime (see Fig. 3 in Ref. 22). On the contrary, their dependence on V is remarkable. These values are shown in Fig. 5. First, we mention that, for $V/W \rightarrow 0$, U_{df}^c tends to a nonzero value ($U_{df}^c/W \approx 0.17$), which indicates that there has to be a finite value of U_{df} even for weak hybridizations to
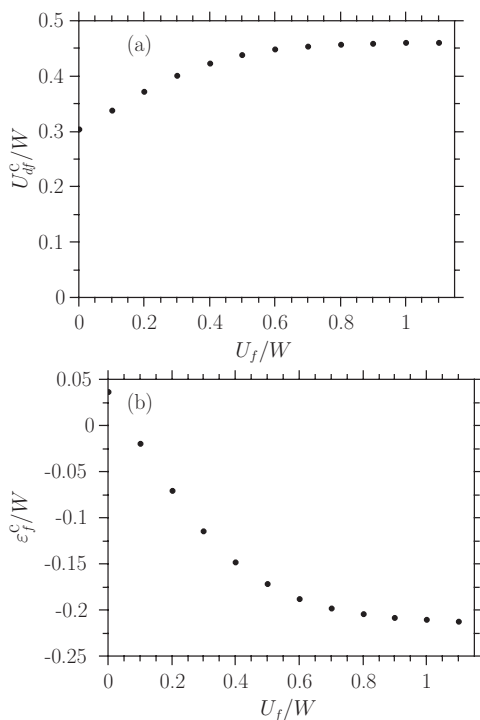

FIG. 4. Panel (a) shows the critical value of U_{df} where the QCP appears as a function of U_f. Panel (b) shows the critical value of ε_f, $V/W = 0.1$ in all cases.
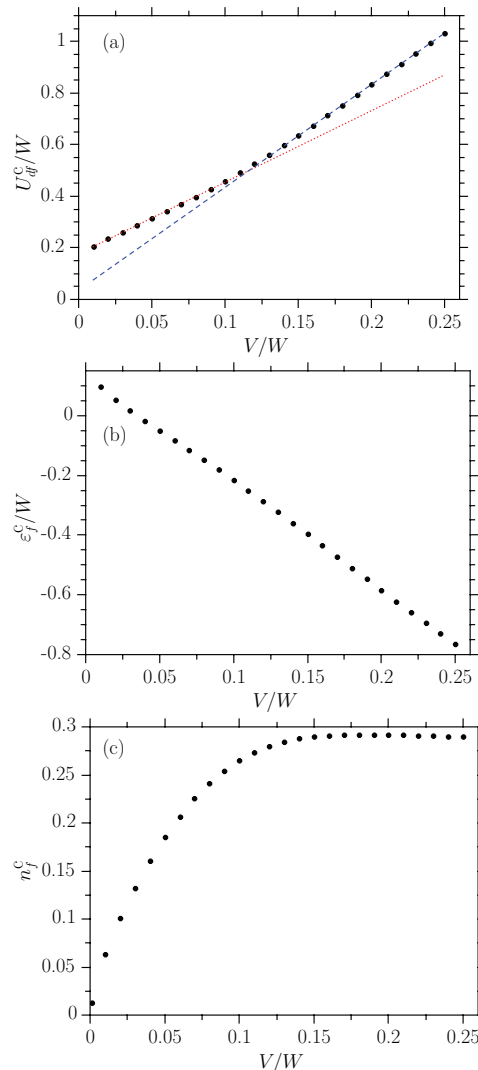

FIG. 5. (Color online) Panel (a) shows the critical value of U_{df} (●) where the QCP appears as a function of the hybridization. The red dotted and blue dashed lines are linear fits to the beginning and to the end of the data, respectively. Panels (b) and (c) show the critical values of ε_f and n_f, respectively; $U_f/W = 3$ in all cases.

obtain a valence transition. The critical position of the f level decreases linearly with increasing hybridization. The critical value of the occupancy of the f level increases from $n_f^c = 0$ at $V = 0$ and saturates as soon as ε_f^c reaches the bottom of the conduction band. Roughly at the same mixing V, the slope of the U_{df}^c-V curve shows a substantial change.

For larger values of U_{df}, two subsequent first-order transitions—from $n_f \approx 2$ to $n_f \approx 1$ (Kondo regime) and from $n_f \approx 1$ to $n_f \approx 0$—take place as ε_f is varied. Their positions are symmetric with respect to $-U_f/2$. This is confirmed by the fact that near the transition a hysteresis is observed, that is, there is a narrow range of ε_f, where two solutions of the variational equations coexist. Therefore, the transition line is identified from the ground-state energy, where the energies of the different configurations are equal.

For even larger values of U_{df}, the width of Kondo regime decreases and at U_{df}^{triple} it ends in a triple point. At the triple point, the energy of the Kondo-like state becomes equal to the
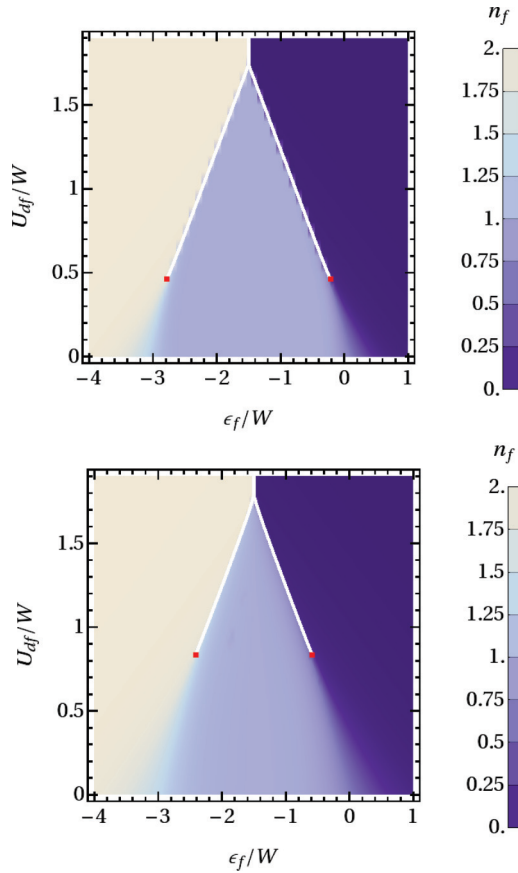
FIG. 6. (Color online) The upper panel shows the ε_f–U_{df} phase diagram for $U_f/W = 3$ and $V/W = 0.1$, while the lower one shows that for $U_f/W = 3$ and $V/W = 0.2$. The solid white lines denote the first-order transition lines. The QCPs are marked by red squares. The point where the white lines meet is the triple point (see the text).

energy of the states with $n_f \approx 2$ and $n_f \approx 0$; therefore, here three different states coexist. We found that the triple point is located at $\varepsilon_f^{\mathrm{triple}} = -U_f/2$ and $U_{df}^{\mathrm{triple}} \approx U_f/2 + W/4$, if there is a Kondo plateau. For small U_f (including $U_f = 0$), when there is no Kondo plateau, the numerical results can be fitted to $U_{df}^{\mathrm{triple}} \approx U_f/2 + W/3$. In Ref. 16, using dynamical mean-field theory, it was found that the Kondo regime is stable for $U_{df} \lesssim U_f/2$. Our result is in agreement with this. The mean-field theory gives similar results except for $U_f = 0$, where the triple point does not exist. Now we can draw the ε_f–U_{df} phase diagram. The results are shown in Fig. 6, using a color code, for two different values of the hybridization and demonstrates our statements described above. The figure demonstrates that the interval of ε_f, where first-order transition occurs, is shortened for larger values of the hybridization.

IV. COMPARISON WITH THE MEAN-FIELD APPROACH AND EXACT DIAGONALIZATION

The mean-field theory and the Gutzwiller approach yield surprisingly close results for $U_{df}/W = 0$ and 1, which is shown in Fig. 7 for a special choice of the parameters. However, the mean-field results show a jump in the f-level occupancy at such small values of U_{df}, where the Gutzwiller method
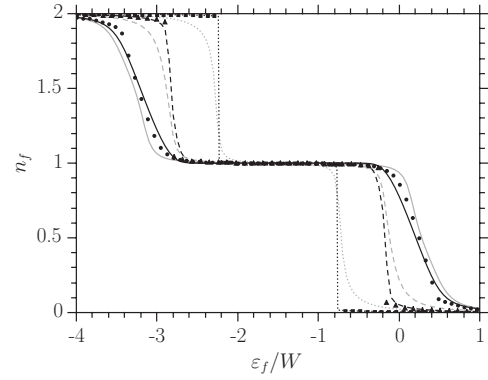

FIG. 7. The f-level occupancy as a function of ε_f. The black curves are obtained from the Gutzwiller method, while the gray ones are calculated from exact diagonalization and the symbols are the results of the mean-field calculation. The solid, dashed, and dotted lines (and the symbols ●, ▲, ■) belong to $U_{df}/W = 0$, 0.4, 1, respectively; $V/W = 0.1$ and $U_f/W = 3$ in all cases.

still gives a continuous change of n_f. The estimated critical value (U_{df}^{c}) from mean-field theory is significantly smaller than that from the Gutzwiller method. It is worth emphasizing that the jump in the mean-field results is due to a level crossing between a paramagnetic and a magnetically ordered state. In contrast, the Gutzwiller method gives a valence transition between paramagnetic states. Both methods result in a triple point for a certain value of U_{df}, and we found that both of them gives $U_{df}^{\mathrm{triple}} \approx U_f/2 + W/4$. For small values of U_f the scenario is the same in both methods as in the large U_f case; however, the values of U_{df}^{triple} and U_{df}^{c} somewhat differ. The only exception is $U_f = 0$, where there is no triple point in the mean-field calculation due to the missing of a stable magnetic solution. Here a direct first-order transition takes place between the nearly fully occupied and nearly empty f levels.

As a further check of our results, we performed exact diagonalization on a one-dimensional chain. Due to the limitation to relatively short chains containing six sites, we do not expect to find critical behavior in this calculation. However, some other features of the effect of U_{df} might be observable. The comparison is shown in Fig. 7. The width of the Kondo plateau is the same using all the three methods; therefore, its shrinking due to U_{df} is not an artifact of the Gutzwiller approximation or the mean-field treatment. Furthermore, by increasing U_{df}, the intermediate valence regime becomes narrower in the exact diagonalization, too, although there is naturally no sharp valence transition.

V. CONCLUSIONS

We have performed mean-field calculation, variational calculation using the Gutzwiller method, and exact diagonalization for the extended PAM, where an additional local Coulomb interaction between the d and f electrons has been included. Earlier calculations found a sharp, first-order valence transition and a critical point at some value of U_{df} for large or infinite U_f couplings. We have generalized the Gutzwiller

method for arbitrary U_f in order to study the small U_f regime and to analyze how the QCP depend on U_f and V.

Both the mean-field theory and the Gutzwiller method have resulted in two subsequent first-order valence transitions as the position of the f level is varied above a critical value of U_{df}, and two QCPs appear in the ε_f–U_{df} plane. We have analyzed variationally the critical behavior as a function of hybridization, the bare f-level energy, and U_f, and have drawn the ε_f–U_{df} phase diagram. It has been pointed out that the Kondo regime shrinks by increasing U_{df}, and ends in a triple point, which obviously cannot be seen in the infinite U_f case. For even larger values of U_{df} a direct first-order

valence transition takes place from $n_f \approx 2$ to $n_f \approx 0$. This can be interpreted as valence skipping, which so far has been attributed to the presence of a negative U_f. We find it for $U_f > 0$, when U_{df} is large enough. The shrinking of the Kondo regime and the narrowing of the intermediate valence regime have been confirmed by exact diagonalization, although naturally, no sharp valence transition is found in finite chains.

[1]N. D. Mathur *et al.*, Nature **394**, 39 (1998).

[2]K. Miyake, S. Schmitt-Rink, and C. M. Varma, Phys. Rev. B **34**, 6554(R) (1986); D. J. Scalapino, E. Loh, Jr., and J. E. Hirsch, *ibid.* **34**, 8190 (1986); P. Monthoux and G. G. Lonzarich, *ibid.* **59**, 14598 (1999).

[3]E. Vargoz and D. Jaccard, J. Magn. Magn. Mater. **177–181**, 294 (1998).

[4]Y. Onishi and K. Miyake, J. Phys. Soc. Jpn. **69**, 3955 (2000).

[5]K. Miyake and H. Maebashi, J. Phys. Soc. Jpn. **71**, 1007 (2002).

[6]H. Q. Yuan *et al.*, Science **302**, 2104 (2003).

[7]A. T. Holmes, D. Jaccard, and K. Miyake, Phys. Rev. B **69**, 024508 (2004).

[8]H. Q. Yuan, F. M. Grosche, M. Deppe, G. Sparn, C. Geibel, and F. Steglich, Phys. Rev. Lett. **96**, 047008 (2006).

[9]S. Watanabe, M. Imada, and K. Miyake, J. Phys. Soc. Jpn **75**, 043710 (2006); J. Magn. Magn. Mater. **310**, 841 (2007).

[10]A. T. Holmes, D. Jaccard, and K. Miyake, J. Phys. Soc. Jpn. **76**, 051002 (2007).

[11]K. Miyake, J. Phys.: Condens. Matter **19**, 125201 (2007).

[12]K. Fujiwara *et al.*, J. Phys. Soc. Jpn. **77**, 123711 (2008).

[13]E. Lengyel, M. Nicklas, H. S. Jeevan, G. Sparn, C. Geibel, F. Steglich, Y. Yoshioka, and K. Miyake, Phys. Rev. B **80**, 140513(R) (2009).

[14]J. P. Rueff, S. Raymond, M. Taguchi, M. Sikora, J. P. Itie, F. Baudelet, D. Braithwaite, G. Knebel, and D. Jaccard, Phys. Rev. Lett. **106**, 186405 (2011).

[15]For reviews on this topic see, for example, P. Fulde, J. Keller, and G. Zwicknagl, in *Solid State Physics: Advances in Research and Applications*, edited by H. Ehrenreich and D. Turnbell (Academic Press, San Diego, 1988), Vol. 41, pp. 1–150; P. Fazekas, *Lecture Notes on Electron Correlation and Magnetism* (World Scientific, Singapore, 1999); A. C. Hewson, *The Kondo Problem to Heavy Fermions* (Cambridge University Press, Cambridge, 1993); H. Tsunetsugu, M. Sigrist, and K. Ueda, Rev. Mod. Phys. **69**, 809 (1997).

[16]Y. Saiga, T. Sugibayashi, and D. S. Hirashima, J. Phys. Soc. Jpn. **77**, 114710 (2008).

[17]T. Yoshida, T. Ohashi, and N. Kawakami, J. Phys. Soc. Jpn. **80**, 064710 (2011).

[18]T. Yoshida and N. Kawakami, Phys. Rev. B **85**, 235148 (2012).

[19]K. Kubo, J. Phys. Soc. Jpn. **80**, 114711 (2011).

[20]V. N. Phan, A. Mai, and K. W. Becker, Phys. Rev. B **82**, 045101 (2010).

[21]T. Sugibayashi, Y. Saiga, and D. S. Hirashima, J. Phys. Soc. Jpn. **77**, 024716 (2008).

[22]I. Hagymási, K. Itai, and J. Sólyom, Phys. Rev. B **85**, 235116 (2012).

[23]A. Koga, N. Kawakami, R. Peters, and T. Pruschke, Phys. Rev. B **77**, 045120 (2008).

[24]I. Hagymási, K. Itai, and J. Sólyom, Acta Phys. Pol. A **121**, 1070 (2012).

[25]C. M. Varma, Phys. Rev. Lett. **61**, 2713 (1988).

[26]K. Itai and P. Fazekas, Phys. Rev. B **54**, 752(R) (1996).